Aalborg Universitet

A Lifetime Prediction Method for LEDs Considering Real Mission Profiles

Qu, Xiaohui; Wang, Huai; Zhan, Xiaoqing; Blaabjerg, Frede; Chung, Henry Shu-hung

A Lifetime Prediction Method for LEDs Considering Real Mission Profiles

Xiaohui Qu, *Member, IEEE,* Huai Wang, *Member, IEEE,* Xiaoqing Zhan, *Student Member, IEEE,*
Frede Blaabjerg, *Fellow, IEEE,* and Henry Shu-Hung Chung, *Fellow, IEEE*

Abstract—The Light-Emitting Diode (LED) has become a very promising alternative lighting source with the advantages of longer lifetime and higher efficiency than traditional ones. The lifetime prediction of LEDs is important to guide the LED system designers to fulfill the design specifications and to benchmark the cost-competitiveness of different lighting technologies. However, the existing lifetime data released by LED manufacturers or standard organizations are usually applicable only for some specific temperature and current levels. Significant lifetime discrepancies may be seen in the field operations due to the varying operational and environmental conditions during the entire service time (i.e., mission profiles). To overcome the challenge, this paper proposes an advanced lifetime prediction method, which takes into account the field operation mission profiles and also the statistical properties of the life data available from accelerated degradation testing. The electrical and thermal characteristics of LEDs are measured by a T3Ster system, used for the electro-thermal modeling. It also identifies key variables (e.g., heat sink parameters) that can be designed to achieve a specified lifetime and reliability level. Two case studies of an indoor residential lighting and an outdoor street lighting application are presented to demonstrate the prediction procedures and the impact of different mission profiles on the lifetime of LEDs.

Index Terms—LED lighting, lifetime prediction, mission profile, reliability.

I. INTRODUCTION

POWER Light-Emitting Diodes (LEDs) are increasingly applied for indoor and outdoor lighting applications due to their higher efficiency and longer lifetime compared to the traditional lighting sources. The lifetime of LED lamps involving LED drivers and source packages is routinely quoted as 25,000 to 50,000 hours in the market [1]–[3]. These claimed lifetimes are usually released by the LED manufacturers or standard organizations. However, the customer experiences may be different and some of the LED lamps can fail in a considerable time ahead of the claimed life [4] [5]. The

X. Qu is with the School of Electrical Engineering, Southeast University, Nanjing, 210096, China. (Email: xhqu@seu.edu.cn)

H. Wang and F. Blaabjerg are with Center of Reliable Power Electronics (CORPE), Department of Energy Technology, Aalborg University, Denmark. (Email: hwa@et.aau.dk; fbl@et.aau.dk)

X. Zhan and H. S. H. Chung are with Center for Smart Energy Conversion and Utilization Research, City University of Hong Kong, Hong Kong. (Email: xiaoqingzhan1011@gmail.com; eeshc@cityu.edu.hk)

failure could be induced either by the LED drivers or by the LED source packages. The discrepancies between the claimed lifetime and the field operation experiences are mainly due to the following reasons [6], [7]:

1) The definition of the specified lifetime of LED lamps is vague. A necessary lifetime definition should include at least four aspects: a) operation conditions; b) end-of-life criteria; c) required minimum reliability at the end of the specified lifetime; d) confidence level of the specified lifetime.
2) The claimed lifetime is usually tested or predicted under a specific temperature and current level. The environmental and operational conditions in field operation may vary within the operation specifications of the LED lamps, or even exceed the specifications for severe users.
3) The lifetime mismatch between the LED drivers and the LED packages may occur. Sometimes, the lifetime of LED packages is misused as the claimed lifetime of the whole LED lamps.

The LED lamps could fail due to the following reasons: 1) failure of LED drivers; 2) catastrophic failure of LED package; and 3) wear out failure due to long-term lumen depreciation and color shift [8]. The level of lumen depreciation is usually used as an end-of-life criteria. For color quality critical applications, the color shift level is also used as an additional criteria. Fig. 1 (a) illustrates the definition of the time to failure L_p of an LED individual. For example, L_{70} is the time when the lumen is maintained at 70% of its initial value. With a more stringent requirement on lumen maintenance, the lifetime is shortened (e.g., L_{90} is less than L_{70} for a specific LED). Nowadays, the L_{70} or L_{85} criteria are usually used for commercial and residential outdoor applications and L_{90} is for residential indoor applications [9]. In some applications without the stringent lumen requirement, L_{50} is also used as a design criteria.

It is known that the L_p lifetime varies among LED samples even with the same part number from the same manufacturer due to the variances in materials, process control, etc [10]. Therefore, the percentile lifetime B_X for a population of LEDs is of more interest with $X\%$ of failures as a result of gradual loss of luminous flux. Fig. 1 (b) shows the definition of B_X lifetime based on the required minimum reliability level R $(= 1 - X\%)$ at the end of the specified lifetime. For example, B_{10} lifetime means the time when 10% of the LEDs fail (i.e., with a reliability $R = 0.9$), and B_1 lifetime

means the time when 1% of the LEDs fail. Accordingly, $L_p B_X$ lifetime refers to the time when $X\%$ of the LEDs have the lumen output below $p\%$ with respect to their initial values. The choices of p and X are application-dependent. $L_p B_X$ lifetime is more legitimate to declare the lifespan of the LED package [11]. It is also applicable for LED drivers to evaluate the reliability level. The reliability curve can be plotted using these L_p data arranged by a specific rank method to define the cumulative percentage of the population. Among different data rank methods as discussed in [12], the median rank is corresponding to a confidence level of 50%. It is also possible to obtain the reliability range with certain Confidence Bounds (CBs) as shown in Fig. 1 (b) with other data rank methods. For example, the 2-sided 90% CBs have the top CB and the bottom CB curve to provide 5% and 95% confidence respectively. These statistical properties are necessary to define the lifetime of LED lamps.

Degradation testing is usually performed to obtain the time to failure L_p of each individual LED sample. The industry standard LES LM-80 [13] requires a minimum of 6,000 hours of degradation testing. LED manufacturers usually conduct the test for 6,000 hours up to 10,000 hours. Based on the available lumen degradation data, the time-to-failure of each testing sample is projected by an exponential curve-fitting extrapolation as described in the standard IES TM-21 [14]. However, TM-21 uses the average degradation value of the LED samples for the further projection, which ignores the statistical properties and therefore the reliability information can not be obtained from the TM-21 procedure. The degradation testing presented in IES LM-80 is usually performed under several specific conditions, that are typical constant driving currents and at least three cases of ambient temperatures (55°C, 85°C and one selected by the manufacturers). The driving current depends on the user profiles and driving schemes. The ambient temperature may vary with time and is geographically dependent. Only one constant current and temperature based reliability prediction method can not take into account a realistic mission profile with loading variations [5], [15]. Therefore, there are still gaps between the degradation testing data and the practical applications like:

1) The specific reliability information (with a certain confidence level or confidence bounds) and the corresponding lifetime model are not readily available. A comprehensive analysis on those testing data is needed.
2) The mapping of the reliability under the specific accelerated testing conditions to under field conditions (i.e., long-term mission profiles) is missing.

To overcome the above issues, this paper proposes an advanced lifetime prediction method concerning the long-term field operation mission profiles and the statistical properties of the life data available from the accelerated degradation testing. The mission profile dependent lifetime models has been analyzed in the conference paper [16], based on the degradation testing data. In this paper, the electrical and thermal characteristics of LEDs are experimentally measured by a Thermal Transient Tester (T3Ster) system, used for the electro-thermal modeling. More temperature steps are used to
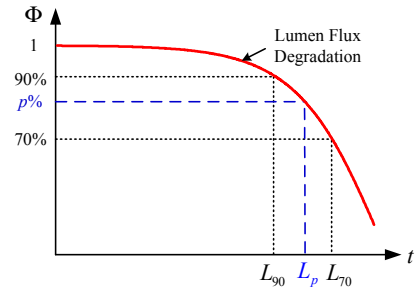
(a) Time to failure L_p of an individual LED
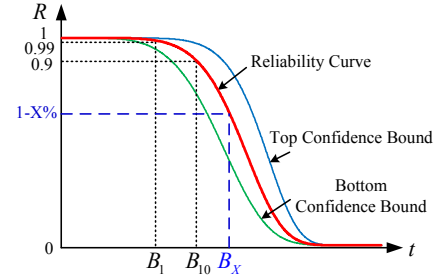
(b) B_X lifetime for a population of LEDs

Fig. 1.   Two LED lifetime criteria, where (a) L_p is defined as the time when $p\%$ of the initial output lumen of an LED is maintained, and (b) B_X is defined as the time when $X\%$ of the LEDs have the lumen output below $p\%$ of their initial values.

obtain the temperature-dependent electro-thermal parameters. A feedback implementation system of the junction temperature to update the electro-thermal parameters is built to acquire the operation point for the accurate lifetime prediction. With the improved electro-thermal models and the lifetime prediction method, some key variables for thermal design and lifetime-matching of LED drivers in different field conditions can easily be identified to achieve a specified lifetime and reliability. Two case studies of an indoor residential lighting application and an outdoor street lighting application are presented to demonstrate the prediction procedures and the impact of different mission profiles on the lifetime of LEDs. The proposed method can also be extended to the prediction of the LED drivers and the entire LED lighting systems.

Specifically, Section II introduces the comprehensive lifetime models involving the statistical properties and the reliability information of life data. Based on these models, an advanced lifetime prediction method is then presented in detail to map the lifetime from the testing condition to the field condition in Section III. Two case studies are demonstrated and evaluate the performance of the proposed method in Section IV. Section V concludes the paper.

II. LIFETIME MODELS AND DEGRADATION TESTING DATA ANALYSIS

Since LEDs are basically *p-n* junctions, the emitted lumen flux and intensity are proportional to the concentration of carriers [17]. The concentration of carriers depends on the current density and junction temperature, which results in LED output lumen, color chromaticity, and the forward voltage characteristics also varying with these two stresses. Hence, a

generally accepted Black model in (1) is used to describe the Time to failure under different stresses [18], [19].

$$\text{Time to failure} = A_0 J^{-n} e^{\frac{E_a}{k_B T}}, \qquad (1)$$

where A_0 is a constant, J is the current density, n is a scaling factor, E_a is the activation energy in unit of eV, k_B is the Boltzmann constant, and T is the absolute temperature in Kelvin.

The model in (1) describes the impact of current and temperature on the lifetime of LEDs. Therefore, L_p lifetime, defined as time to failure for an LED individual, follows this model. Moreover, B_X lifetime based on a population of L_p lifetime data also follows this equation to specify the reliability of an LED population. The parameters of A_0, n and E_a are usually obtained according to the accelerated testing data. n and E_a are material-dependent, which can be assumed constant for a given type of LEDs with a given failure mechanism. Hence, (1) can be rearranged as (2) and (3).

$$L_p(I_F, T_J) = A_p I_F^{-n} e^{\frac{E_a}{k_B T_J}}, \text{ and} \qquad (2)$$

$$B_X(I_F, T_J) = A_X I_F^{-n} e^{\frac{E_a}{k_B T_J}}, \qquad (3)$$

where I_F is the LED driving current proportional to the current density, and T_J is the junction temperature of LEDs. Although A_p and A_X are dependent on the different L_p and B_X criteria, (2) and (3) have the same Acceleration Factors (AF).

$$AF(n, E_a) = \left(\frac{I_F}{I_{F0}}\right)^{-n} e^{\frac{E_a}{k_B}\left(\frac{1}{T_J} - \frac{1}{T_{J0}}\right)}. \qquad (4)$$

Here, (I_{F0}, T_{J0}) is the initial stress level, whilst (I_F, T_J) is the accelerated stress level. To solve factors of n and E_a in (4), the time-to-failure data from at least three different stress levels are required.

With this information, a case study based on an LM-80 test report [20] for Lumileds Luxeon Rebel LEDs [21] will show how to establish the models of (2) and (3), where the data in the LM-80 report are experimentally measured by the manufacturers. Weibull distribution is the most widely used to process the lifetime data in reliability engineering [12], which is adopted here to analyze the reliability information of LEDs. The report [20] provides multiple accelerated life testing conditions with stress levels of I_F from 0.35 A, 0.5 A, 0.7 A, to 1 A and air temperature T_a from 55°C, 85°C, 105°C, to 120°C. There are 25 samples in each test to ensure the accurateness of the results, lasting for at least 9,000 hours. To solve n and E_a in (4), at least three different stress levels of I_F and T_J are randomly chosen. Here, the degradation data and fitted curves at three stress levels of I_F and T_J with (0.35 A, 129°C), (0.7 A, 74°C) and (1 A, 112°C) are plotted by software tool *ReliaSoft* [22] and shown in Fig. 2. The data points are provided by LM-80 report, which are measured every 1,000 hour for 25 samples in the accelerated testing. Then the fitting curves are projected by an exponential extrapolation according to TM-21 procedure. With two end-of-life criteria L_{70} and L_{90}, two groups of end-of-life L_p data can be read directly in Fig. 2. It should be noted that TM-21 uses the average lumen value of the samples for the further projection, which ignores the statistical properties and provides
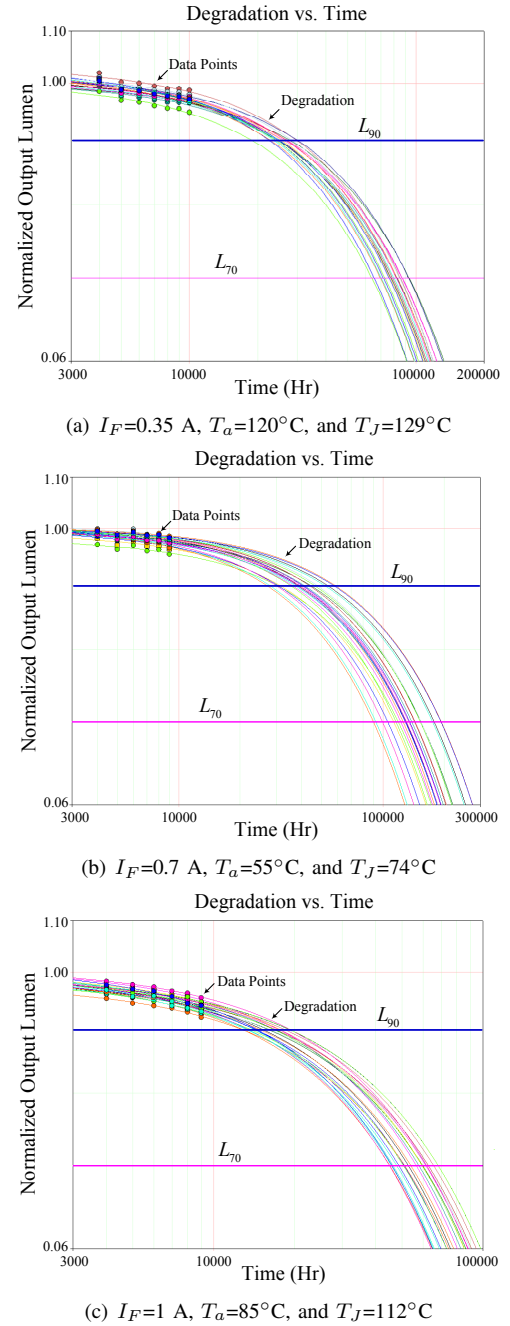
Fig. 2. Lumen degradation curves with L_{70} and L_{90} lifetime criteria under different LED operating conditions of (a), (b) and (c). X-axis is time in hour of logarithmic scale and Y-axis is the normalized output lumen with respect to the initial lumen at $t=0$.

limited information. Therefore, the long-term lumen projection is done for each sample in the proposed method.

Each group of L_p data is then arranged in sequence and ranked by the algebraic approximation of the Median rank in (5) [12].

$$\text{Median rank } r_j = \frac{j - 0.3}{N + 0.4}, \qquad (5)$$

where j is the order number of the sequenced L_p data, $j \in [1, N]$ and N is the total number of failure (i.e., the size of L_p data). The rank r_j is actually the probability to failure for

the jth LED. With these ranks and the corresponding L_p group at one stress level, the probability to failure line for this stress level can be generated via *ReliaSoft ALTA* (Accelerated Life Testing Analysis) degradation. Figs. 3 (a) and (b) illustrate the unreliability function $F(t)$ (i.e., probability to failure function) at each operating stress level with 50% confidence level. The unreliability curves with the different confidence levels could also be plotted upon the application requirements. In Figs. 3 (a) and (b), most data points of the three stress groups are fitted to the Weibull distribution reasonable well. Few data points outside of the probability lines due to the measurement error or LED sample variation can be dismissed here. With the three probability lines, B_X satisfying $F(B_X) = X\%$ can be obtained. The probability lines follow the two-parameter Weibull distribution and the cumulative failure $F(t)$ is described as

$$F(t) = 1 - R(t) = 1 - e^{-(\frac{t}{\eta})^{\beta}}, \tag{6}$$

where t is time, β is the shape parameter, and η is the scale parameter of characteristic life $B_{63.2}$ (i.e., the life at which 63.2% of the tested samples fail) at each stress condition. For the wear-out failure, $\beta > 1$. With the same failure mechanism, β is assumed constant under different stress levels within the physical limits [12]. In Figs. 3 (a) and (b), six well fitted curves show good consistence on β, n and E_a, where the discrepancies are caused by the distribution variation. Besides, the probability lines under the different stress levels can be readily plotted in the figure with the same β, n, E_a and different η, such as two lines at the stress level of I_F and T_J with (0.7 A, 25°C, i.e., 298 K) in Figs. 3 (a) and (b) seperately.

With the known n and E_a, substituting any B_X value at one stress (I_F, T_J) into (3), A_X can be solved. Two groups of n and E_a are derived from the experimental accelerated testing data, and can be validated by the good consistence. Thus, any percentile B_X lifetime with different failure rate $X\%$ can be derived using the above mentioned method. Here, B_{10} and B_1 distributions based on L_{70} and L_{90} criteria are given in (7) and Fig. 4 as examples, which are valuable for further mapping the reliability information under field operational mission profiles, and discussed in the next section.

$$\begin{cases} \ln B_{10\_L70}(I_F, T_J) = 3.956 - 0.57 \ln I_F + \dfrac{2588}{T_J} \\[2mm] \ln B_{1\_L70}(I_F, T_J) = 3.628 - 0.57 \ln I_F + \dfrac{2588}{T_J} \\[2mm] \ln B_{10\_L90}(I_F, T_J) = 2.558 - 0.698 \ln I_F + \dfrac{2636}{T_J} \\[2mm] \ln B_{1\_L90}(I_F, T_J) = 2.221 - 0.698 \ln I_F + \dfrac{2636}{T_J} \end{cases} \tag{7}$$

III. Experimental Characterization of Electro-Thermal Properties of LEDs and Mission Profile Based Lifetime Prediction

From Fig. 4, I_F and T_J are the key factors to predict the lifetime and reliability in the LED lighting applications. In the field operation, the LED driving current I_F depends on
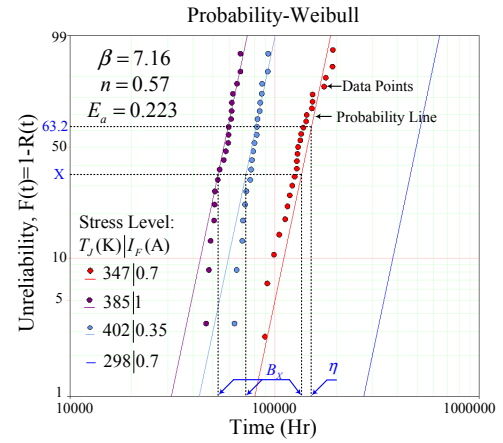
(a) With L_{70} criteria
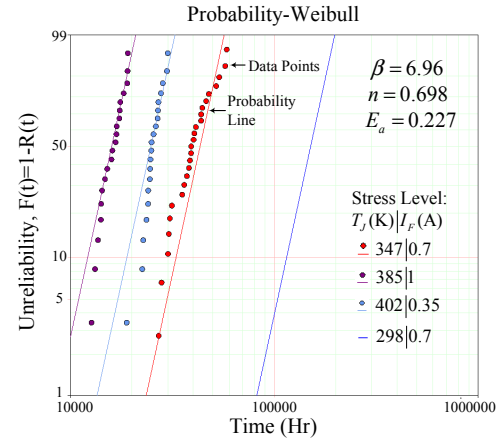
(b) With L_{90} criteria

Fig. 3. Unreliability curves under different stress levels based on the L_p data given in Fig. 2. X-axis is time in hour of $\ln(t)$ scale and Y-axis is percentage in the scale of $\ln \ln(\frac{1}{1-F(t)})$.
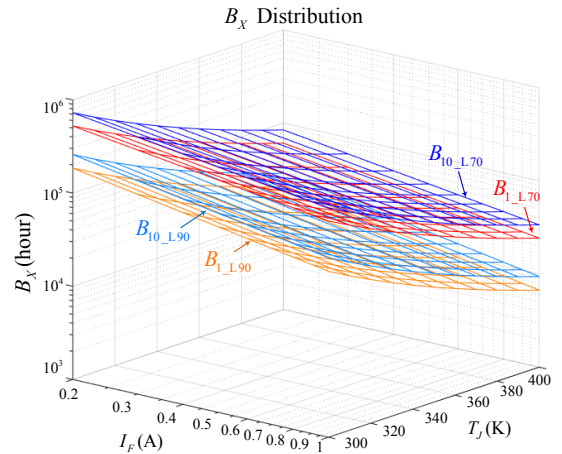

Fig. 4. B_X lifetime vs. forward current I_F and junction temperature T_J.

the user profiles (e.g., indoor or outdoor occasion for different lumen requirements, dimming schemes, and periodical operational hours per day, month or year, etc.). The junction temperature T_J, which is affected by the ambient temperature T_A, power loss in chip, and thermal distribution of materials,
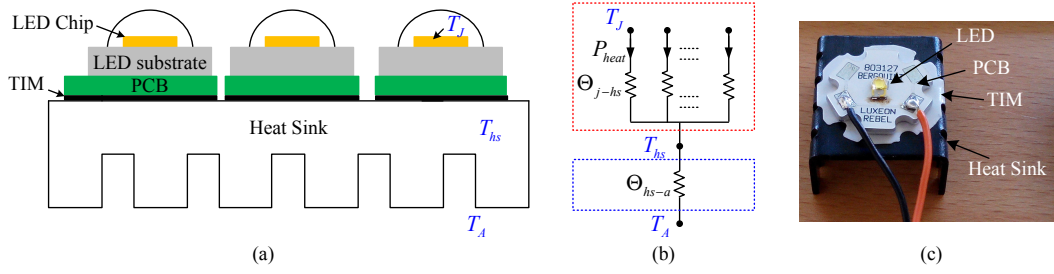
Fig. 5. (a) A typical LED package structure with (b) the equivalent thermal circuit and (c) the practical package example.

cannot be measured directly. Although there are some methods to estimate T_J by using temperature-sensitive electrical parameters, considerable implementation efforts are necessary [23], [24]. Therefore, the junction temperature estimation based on the accurate electro-thermal model with the help of updating of field operation conditions is a feasible way to analyze the long-term thermal profiles in this study.

A. LED Electro-Thermal Model

It is known that most energy of LEDs is converted to heat and the left energy is converted into visible radiant light energy. The heat in the LED die can be diffused only by the heat sink or external cooling, whereas the conventional light sources can emit most heat by radiation. Fig. 5 (a) shows a typical structure of an LED package, where multiple LED dies are soldered on the individual PCB substrate for electrical connection, and the PCB is then attached to a heat sink for the further heat conduction. To maximize the heat transfer between the heat sink and the PCB, a Thermal Interface Material (TIM) is needed to fill the air voids. Then the heat can be conducted from the inner *p-n* junction via substrate, cladding layer, PCB, and TIM to the heat sink and then radiated and convected to the ambient air. Using Cauer thermal model [25], it can be described in Fig. 5 (b), where P_{heat} is the dissipated heat power by each LED die. Θ is the thermal resistor of each layer in $\frac{^{\circ}C}{W}$ or $\frac{K}{W}$ determined by the material and geometry of this layer. Here, it should be noted that the thermal capacitors contributed from the chips, packaging and heat sink have not been included in the thermal model because the LED lifetime is determined by the steady-state junction temperature and thus the lifetime consuming during the transient periods of the real mission profiles can be ignored. However, Θ is still dependent of the operation current and temperature [26], [27]. Fig. 5 (c) shows a photo of an LED package as an example to clarify the different layers.

Assuming there are m LEDs being connected in series in one package, which have uniform heat dissipation, it follows (8) in the steady state.

$$T_J(T_A, P_{\text{heat}}, \Theta_{\text{hs}-a}) = T_A + P_{\text{heat}} \cdot \Theta_{\text{j}-a}$$
$$= T_A + P_{\text{heat}} \cdot (\Theta_{\text{j}-\text{hs}} + m\Theta_{\text{hs}-a}), \quad (8)$$

where $\Theta_{\text{hs}-a}$ is thermal design dependent and $\Theta_{\text{j}-\text{hs}}$ is composed of the thermal resistor of each layer including LED junction, PCB and TIM. P_{heat} is caused by non-radiative electron-hole recombination and counts for a large proportion
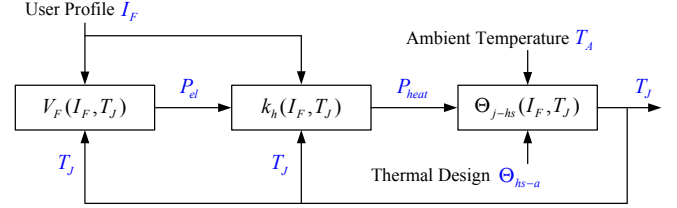

Fig. 6. A flow-chart to update the LED electro-thermal parameters according to the information of the forward current I_F, ambient temperature T_A, and junction temperature T_J.

k_h of the input electrical power P_{el}, which is the product of driving current I_F and diode forward voltage V_F. Thus,

$$P_{\text{heat}} = k_h P_{\text{el}} = k_h I_F V_F. \quad (9)$$

As a semiconductor *p-n* junction, the *V-I* characteristic follows

$$I_F = I_S \left(e^{\frac{eV_F}{Nk_B T_J}} - 1 \right). \quad (10)$$

k_h is not constant for a single LED, varying with T_J and P_{el} [28]. As P_{el} is a function of I_F and T_J, P_{heat} can be calculated as

$$P_{\text{heat}}(I_F, T_J) = k_h(I_F, T_J) \cdot I_F \cdot V_F(I_F, T_J). \quad (11)$$

Comparing (11) and (8), T_J is coupled with P_{heat}, I_F, k_h and $\Theta_{\text{j}-\text{hs}}$. Therefore, a feedback of the junction temperature to update the electro-thermal parameters is necessary in the modeling.

B. Acquisition of Operation Points and Implementation

Based on the Cauer thermal model in (8), Fig. 6 shows a flow chart to take into account the forward current and junction temperature dependent electro-thermal parameters of LEDs. I_F and T_A describe the field operation conditions of LEDs. The thermal heat sink is selected by the LED system designer to fulfill the lifetime and reliability requirement. The key relations of LED *V-I* curve $V_F(I_F, T_J)$, heat coefficient $k_h(I_F, T_J)$, and thermal resistance $\Theta_{\text{j}-\text{hs}}(I_F, T_J)$ are the instinct characteristics of LEDs. The *V-I* curve and thermal resistance are usually shown in the datasheet under some typical testing conditions, e.g., the temperature of thermal pad is kept at 25°C. To predict the lifetime of field operation accurately, more testing conditions will be carried out with the help of the T3Ster system [29], as shown in Fig. 7 (a).
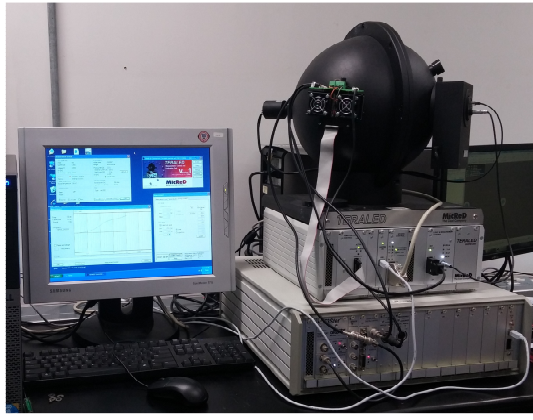
(a)
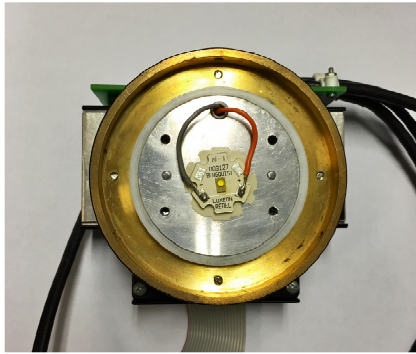
(b)

Fig. 7.   Experimental characterization system: (a) Photo of a T3Ster system, and (b) the LED package in Fig. 5 (c) mounted on a heat plate.

Fig. 8.   Measured *V-I* curves for a Lumileds Luxeon Rebel white LED.
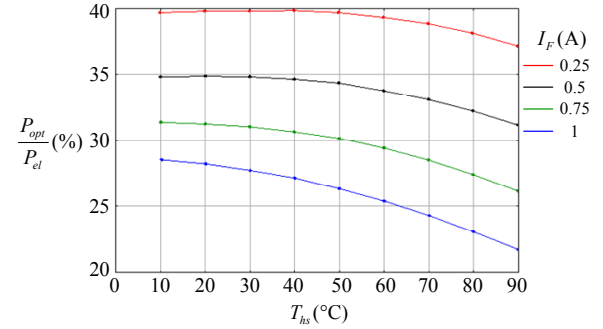
Fig. 9.   Measured wall plug efficiency ($\frac{P_{\mathrm{opt}}}{P_{\mathrm{el}}}$) versus temperature by T3Ster.

T3Ster device can measure the electrical, optical and thermal characteristics of LEDs simultaneously. However, T3Ster system cannot measure the junction temperature directly. From (8), $T_J = T_{\mathrm{hs}} + P_{\mathrm{heat}}\Theta_{\mathrm{j-hs}}$. Then the 3-D relationships of *V-I* curve V_F, heat coefficient k_h, and thermal resistance $\Theta_{\mathrm{j-hs}}$ with respect to junction temperature T_J and driving current I_F in Fig. 6 can be the function of heat sink temperature T_{hs} and driving current I_F. Thus, the LED package in Fig. 5 (c) is mounted on a metal plate as shown in Fig. 7 (b). T3Ster device can readily control the temperature of metal plate, i.e., the heat sink temperature T_{hs}, and then to regulate the junction temperature at different levels. Therefore the feedback signal T_J in Fig. 6 has to change to T_{hs}. The thermal pad with the LED package is put inside the T3Ster test sphere and the driving current is provided by the T3Ster power booster. Then the electro-optical-thermal characteristics with respect to the heat sink temperature and driving current can be measured and obtained directly.

According to the ranges of driving current and ambient temperature, 36 combination of stress levels (i.e., driving current steps of 0.25A, 0.5A, 0.75A, to 1A, and heat sink temperature steps of 10°C, 20°C, $\cdots$, 90°C) are chosen and the corresponding thermal resistances, heat coefficient, and operation points in the *V-I* curves are obtained from experimental measurements, where the measured Lumileds Luxeon Rebel LED has the maximum rating current of 1 A
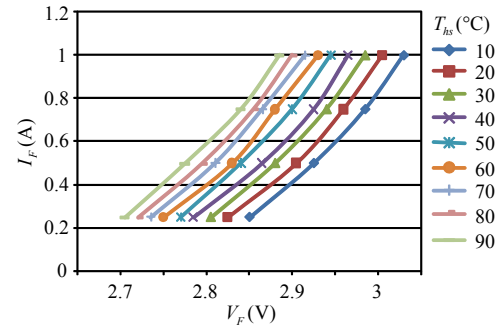
and maximum junction temperature of 150°C. The 36 sets of measured data include the *V-I* characteristics as shown in Fig. 8, and the measured radiated optical power P_{opt} and the ratio of $\frac{P_{\mathrm{opt}}}{P_{\mathrm{el}}}$ at the different stress levels as plotted in Fig. 9. According to (9), $k_h = \frac{P_{\mathrm{heat}}}{P_{\mathrm{el}}} = 1 - \frac{P_{\mathrm{opt}}}{P_{\mathrm{el}}}$. Fig. 10 is the measured cumulative structure function at 10°C of T_{hs} as an example, where the X-axis is the cumulative thermal resistance while Y-axis is the cumulative thermal capacitance. The cumulative thermal resistance starts from the inner LED *p-n* junction, PCB, TIM to the constant ambient thermal pad. The structure function tends to infinity, corresponding to the fact that the universe as a general thermal environment has an infinite thermal capacitance [30]. The distance between the origin and the location of this singularity of the structure function is the thermal resistance $\Theta_{\mathrm{j-hs}}$. These 36 sets of measured data build up three 3-D lookup tables of *V-I* curves, heat coefficient, and thermal resistance, respectively, with respect to heat sink temperature and driving current. By curve fitting of these lookup table data, respective mapping relations are obtained as a function of driving currents and heat sink temperature.

Using these 3-D curves of *V-I*, k_h and $\Theta_{\mathrm{j-hs}}$, Fig. 6 is reconstructed as shown in Fig. 11. Since heat sink temperature can be represented by ambient temperature, heat sink thermal resistance, and dissipated heat power, the forward voltage, heat coefficient, and thermal resistance are further modeled as a function of ambient temperature and driving current. Therefore, for a given instantaneous ambient temperature and driving current mission profiles, the corresponding junction temperature of the LEDs can be obtained [31]. The mission
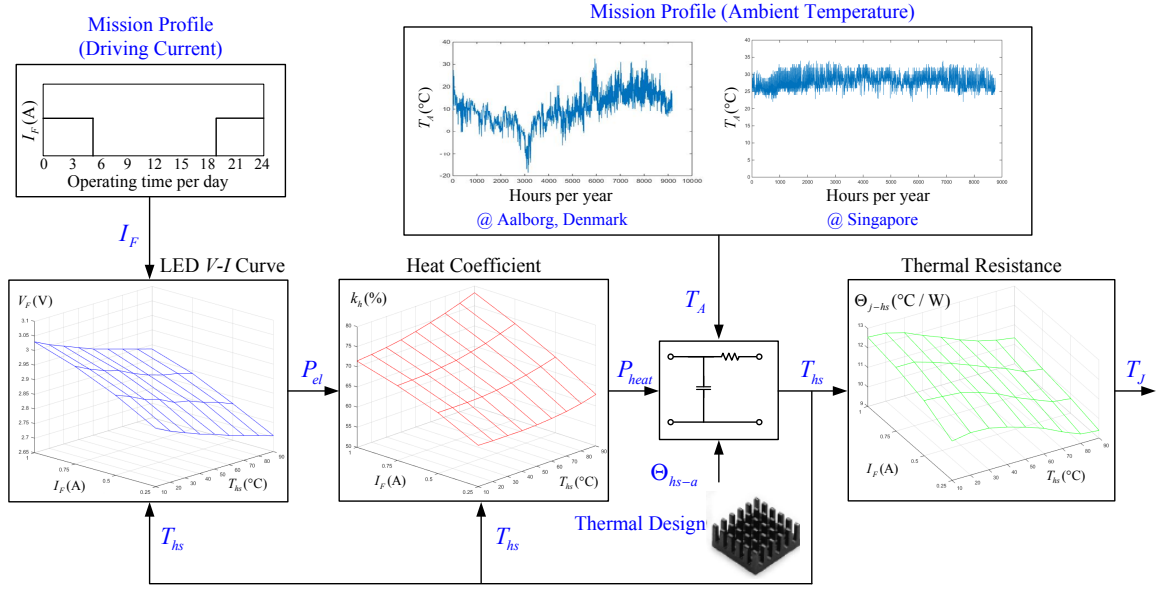
Fig. 11. The implementation of the flow chart in Fig. 6. The mission profiles are for an outside street LED lamp located in Aalborg, Denmark or Singapore.
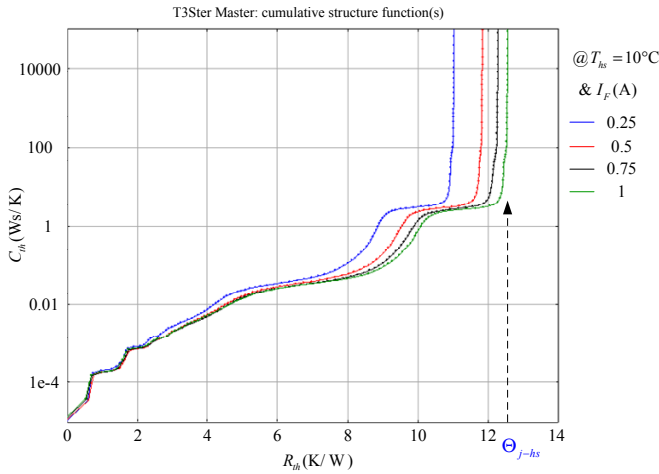

Fig. 10. Cumulative structure function of the heat-flow path. X-axis is the cumulative thermal resistance in $\frac{K}{W}$ while Y-axis is the cumulative thermal capacitance in $\frac{Ws}{K}$. The X-coordinate of the curve singularity corresponds to the thermal resistance $\Theta_{\mathrm{j-hs}}$.

profiles shown in Fig. 11 are of a typical outside street lamp with the light on from 19:00 pm to the next day 5:00 am continuously.

C. Reliability Mapping and Evaluation

For a given operation condition of ambient temperature and forward current, the corresponding B_X lifetime can be predicted. Under the mission profiles with varying ambient and loading conditions, the Consumed Lifetime (CL) can be predicted based on an assumption of linear accumulated damage model (i.e., the Palmgren-Miner model [32]) below:

$$CL = \sum_{i=1}^{k} \frac{t_i}{B_{Xi}}, \qquad (12)$$

where k is the number of different stress levels and t_i is the accumulated duration at the stress $(I_F, T_J)_i$, while B_{Xi} is the B_X lifetime at the stress $(I_F, T_J)_i$. The corresponding B_X lifetime under varying ambient and loading conditions is the time when *CL* reaches 1. The annual profiles shown in Fig. 11 is only a part of the mission profile. Assuming that the conditions are the same from year to year, the B_X lifetime can be calculated by (13).

$$B_X(\mathrm{hour}) = \frac{1}{CL_{\mathrm{year}}} \cdot \text{Service Time (hours per year)}. \quad (13)$$

IV. CASE STUDY AND VALIDATION

To demonstrate the impact of different heat sinks and mission profiles on the lifetime of LEDs, two case studies for an indoor residential lighting application and an outdoor street lighting application in the two cities Aalborg, Denmark and Singapore with very different ambient temperatures are discussed here. The Lumiled Rebel white LEDs are mounted on the heat sinks with different thermal resistances $\Theta_{\mathrm{hs-a}}$. The PCB substrate uses thermally conductive insulated metal substrate from Berquistand [33] and TIM uses very thin thermal pad from t-Global Technology [34], both of which construct $\Theta_{\mathrm{j-hs}}$ with the LED inner junction-to-case thermal resistance. The *V-I* curve, k_h and $\Theta_{\mathrm{j-th}}$ lookup tables of LEDs are measured by T3Ster as shown in Fig. 11. Here, all steps in the lifetime prediction (i.e., mission profiles, electro-thermal models, and lifetime model) are based on experimental results.

A. Indoor Residential Lighting Case

The indoor residential lighting is assumed working in the constant room temperature, 22°C in the cold half year and 26°C in the warm half year from 19:00 pm to 24:00 pm every day. The L_{90} criteria runs here. Firstly, the single LED mounted on the individual heat sink are demonstrated. Using the flow-chart in Fig. 11, T_J can be estimated and then

substituted into Eq. (7) to calculate B_{Xi} at that stress level. The annual lifetime consumption CL_{year} at $\Theta_{\text{hs-a}}$ of 20 °C/W for an example can be calculated as 0.0164 by Eq. (12) and the according B_X is 112,000 hours by assuming that the ambient and loading profiles keep the same from year to year. The predicted lifetime data with different heat sinks are plotted in Fig. 12 (a). The heat sink having a smaller thermal resistance $\Theta_{\text{hs-a}}$ behaves a better thermal performance. To reach the required reliability and lifetime level, the maximum permitted thermal resistance can be read in Fig. 12 (a). It is clear that the B_1 criteria having 99% reliability requires a much better thermal performance than the B_{10} criteria with 90% reliability. For example, a minimum 50,000 hours lifetime with 90% reliability needs the heat sink with a maximum $\Theta_{\text{hs-a}}$ of 76.2 °C/W whilst it needs the better heat sink with a maximum $\Theta_{\text{hs-a}}$ of 51.5 °C/W if 99% reliability applies.

A single LED having about 1 W per chip can not satisfy the lumen requirement in most residential applications. Multiple LEDs are usually connected in series to emit higher lumen. The number of LEDs working together depends on the required power of the different applications. Here, we take a 20 W indoor lamp for example. I_F is set as 0.35 A and the typical forward voltage of the Lumiled Rebel white LED is about 3.3 V at 25°C. Then 18 (= $\frac{20}{0.35*3.3}$) LEDs are mounted together on the same heat sink. Based on (8), $T_J = T_A + P_{\text{heat}} \cdot (\Theta_{\text{j-hs}} + 18\Theta_{\text{hs-a}})$. To show the effect of ambient temperature stress to the B_X lifetime, the 18 LEDs are working at the indoor constant temperature and outdoor two different locations, Aalborg, Denmark and Singapore, respectively. The mission profile in Fig. 11 shows the yearly ambient temperature in Aalborg, Denmark, whilst Singapore has a relatively high temperature all the year with smaller temperature variation. Similarly, Fig. 12 (b) plots the B_{10} lifetimes versus the thermal resistance of heat sink under the same L_{90} criteria and driving current profile. Here, the equivalent thermal resistor of the heat sink for each LED should be $18\Theta_{\text{hs-a}}$, which is consistent with that in Fig. 12 (a). It is clear that the higher ambient temperature will shorten the B_X lifetime. It also provides a guideline for the lamp designers to choose the proper heat sink to fulfill the designed lifetime under a specific mission profile.

B. Outdoor Street Lighting Case

Unlike the indoor application, the street lamp endures the variable outdoor temperatures at different locations. Usually, the outdoor lighting uses the less stringent L_{70} cirteria. The same LED lamp in Fig. 12 (b) works at I_F=0.35 A from 19:00 pm to the next day 5:00 am per day as the street lamp in these two cities Aalborg, Denmark and Singapore. Fig. 13 (a) gives comparison of B_{10} based on L_{70} criteria versus $\Theta_{\text{hs-a}}$ in these two cities. Obviously, the thermal resistor of heat sink is much larger under L_{70} criteria than that under L_{90} criteria in Fig. 12 (b) at each location. To have the same 50,000 hours lifetime, a heat sink with a maximum $\Theta_{\text{hs-a}}$ of 9.08 °C/W is required in Singapore, compared to $\Theta_{\text{hs-a}}$ of 10.6 °C/W required in Aalborg. Fig. 13 (b) also gives the comparison to show the effect of different driving current to
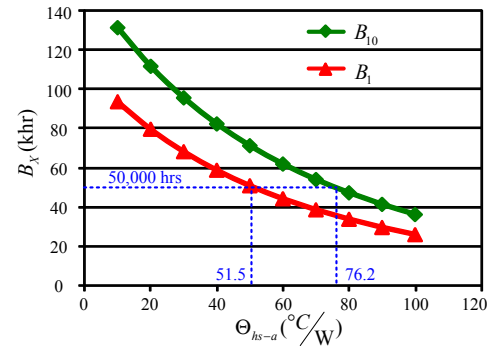
(a) With a single LED
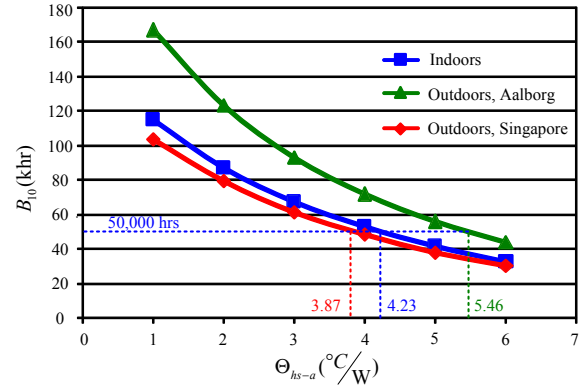
(b) With 18 LEDs mounted together

Fig. 12. B_X lifetime versus $\Theta_{\text{hs-a}}$ of heat sink for indoor residential lamp with L_{90} criteria. (a) A single LED mounted on the single heat sink. (b) 18 LEDs mounted on the same heat sink operating at the indoor and outdoor locations. Y-axis is lifetime in kilo hour (khr).

the B_{10} lifetime, where the LED lamp works at I_F=0.7 A. The larger driving current produces more heat power, and the better heat sink with smaller thermal resistor is required. From these two figures, the impact of the mission profiles of driving current and ambient temperature can be seen on the operation lifetime. Therefore, the same LED products supplied for the different districts and countries of the world must have specific thermal design for the enough lifetime and reliability.

V. CONCLUSION

A mission profile based lifetime prediction method is proposed to estimate the lifetime and reliability performance of LEDs in field operations. It is capable to take into account the impact of long-term field electro-thermal loading stresses to the operating lifetime and reliability. Moreover, the statistic properties of life data from accelerated degradation testing are considered through Weibull analysis to facilitate the lifetime models. This paper also improves the temperature-dependent electro-thermal models using a Thermal Transient Tester system. One study case of an indoor residential lighting application reveals that the LED B_X lifetime could vary with different heat sink thermal resistances. Another specific case of an outdoor street lighting application shows the different predicted lifetime curves under mission profiles in Aalborg and Singapore. The LED manufacturers may follow the proposed lifetime prediction method and provide the system designers
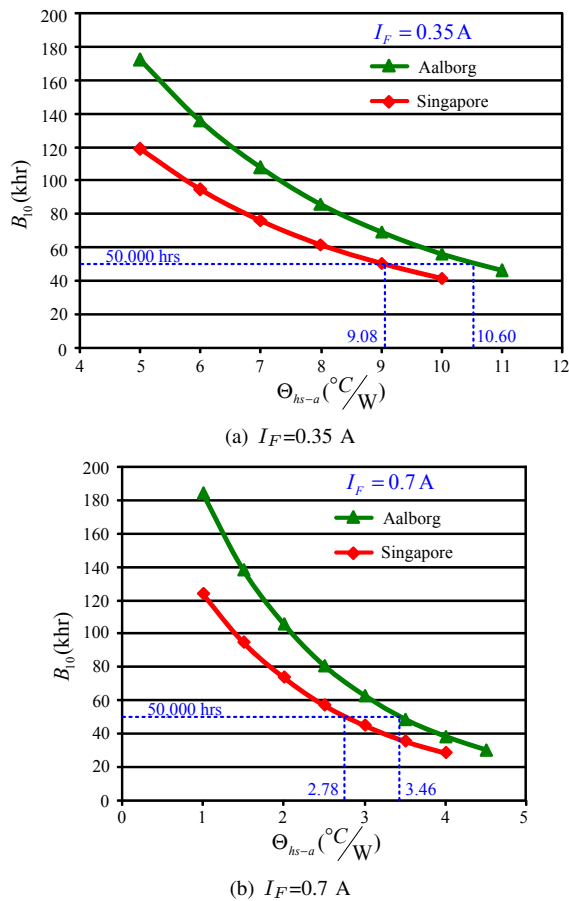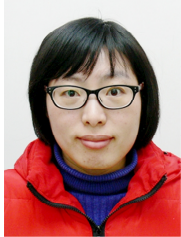
(a) I_F=0.35 A

(b) I_F=0.7 A

Fig. 13. B_{10} lifetime versus Θ_{hs-a} of heat sink for outdoor street lighting with L_{70} criteria when (a)I_F=0.35 A and (b)I_F=0.7 A .

a guideline on the thermal design of LED lighting systems at different locations and a procedure to benchmark different design solutions, taking into account the statistical properties.

REFERENCES

[1] Cree LED lamps,[Online] Available: http://creebulb.com/products.
[2] GE LED lamps,[Online] Available: http://catalog.gelighting.com/lamp/led-lamps/.
[3] Philips lighting,[Online] Available: http://www.lighting.philips.com/main/prof.
[4] Daily Mail Reporter, "The great LED lightbulb rip-off: One in four expensive 'long-life' bulbs doesn't last anything like as long as the makers claim," 2014. [Online] Available: http://www.dailymail.co.uk/news/article-2546363/.
[5] W. D. van Driel and X. J. Fan, "Solid state lighting reliability: Components to systems, " *Springer,* 2013.
[6] H. Wang, M. Liserre, F. Blaabjerg, P. P. Rimmen, J. B. Jacobsen, T. Kvisgaard, and J. Landkildehus, "Transitioning to phyiscs-of-failure as a reliability driver in power electronics," *IEEE Journal of Emerging and Selected Topics in Power Electronics,* vol. 2, no. 1, pp. 97–114, Mar. 2014.
[7] H. S. H. Chung, H. Wang, F. Blaabjerg, and M. Pecht, "Reliability of power electronic converter systems," *The Institution of Engineering and Technology,* 2015.
[8] N. Narendran and Y. Gu, "Life of LED-based white light sources," *IEEE/OSA Journal of Display Technology,* vol. 1, no. 1, pp. 167–171, Sep. 2005.
[9] Department of Energy, U.S., "Lifetime of White LEDs," 2015. [Online] Available: http://apps1.eere.energy.gov/buildings/publications/pdfs/ssl/lifetime_white_leds.pdf.
[10] M. S. Shur and A. Žukauskas, "Solid-state lighting: toward superior illumination," *Proceeding of IEEE,* vol. 93, no. 10, pp. 1691–1703, Oct. 2005.
[11] ZVEI, "Reliable planning with LED lighting," 2016. [Online] Available: http://www.schuch.de/sites/default/files/ZVEI_Planungssicherheit_LED_Englisch _14%2003%2014.pdf.
[12] P. O'Conneor and A. Kleyner, "Practical reliability engineering, 5th Ed.," *John Wiley & Sons,* 2012.
[13] Illuminating Engineering Sciety, "Approved method: measuring lumen maintenance of led light sources," 2008. [Online] Available: https://www.ies.org/store/product/approved-method-measuring-lumen-maintenance-of-led-light-sources-1096.cfm.
[14] Illuminating Engineering Sciety, "Projecting long term lumen maintenance of led light sources," 2011. [Online] Available: https:// www.ies.org/store/product/projecting-long-term-lumen-maintenance-of-led-light-sources-1253.cfm.
[15] J. Fan, K. C. Yung, and M. Pecht, "Lifetime estimation of high-power white LED using degradation-data-driven method," *IEEE Transactions on Device and Materials Reliability,* vol. 12, no. 2, pp. 470–477, Jun. 2012.
[16] X. Qu, H. Wang, X. Zhan, F. Blaabjerg, and H. S. H. Chung, "A lifetime prediction method for LEDs considering mission profiles," *IEEE Applied Power Electronics Conference and Exposition (APEC),* Long Beach, CA, U.S., 2016, pp. 2154–2160.
[17] S. Koh, W. V. Driel, and G. Q. Zhang, "Degradation of light emitting diodes: a proposed methodology," *Journal of Semiconductiors,* vol. 32, no. 1, pp. 014004-1–4, Jan. 2011.
[18] International Sematech Inc., "Semiconductor device reliability failure models," 2000. [Online] Available: http://www.sematech.org/docubase/document/3955axfr.pdf.
[19] C. J. Foo, "White Paper: Calculate the LED lifetime performance in optocouplers to predict reliability," 2014. [Online] Available: http://www.avagotech.com/docs/AV02-3401EN.
[20] Lumileds Inc., "IESNA LM-80 test report," 2012. [Online] Available: http://www.philipslumileds.com/uploads/362/DR05-1-pdf.
[21] Lumileds Inc., "Luxeon Rebel Gerneral purpose white," 2015. [Online] Available: http://www.lumileds.com/uploads/28/DS64-pdf.
[22] ReliaSoft Corp., [Online] Available: http://www.reliasoft.com/.
[23] X. Qu, S. C. Wong, and C. K. Tse, "Temperature measurement technique for stabilizing the light output of RGB LED lamps," *IEEE Transactions on Instrumentation and Measurement,* vol. 59, no. 3, pp. 661–670, Mar. 2010.
[24] D. A. Lock, S. R. G. Hall, A. D. Prins, B. G. Crutchley, S. Kynaston, and S. J. Sweeney, "LED junction temperature measurement using generated photocurrent," *Journal of Display Technology,* vol. 9, no. 5, pp. 396–401, May 2013.
[25] Infineon Inc., "Thermal equivalent circuit models," 2008. [Online] Available: http://www.infineon.com/dgdl/Infineon - AN2008_03_Thermal_equivalent_circuit_models-AN-v1.0-en.pdf?fileId=db3a30431a5c32f2011aa65358394dd2.
[26] L. Jayasinghe, Y. Gu, and N. Narendran, "Characterization of thermal resistance coefficient of high-power LEDs," 2006. [Online] Available: http://lightingresearch.org/programs/solidstate/pdf/jayasinghe-spie6337.pdf.
[27] C. Wang, S. Kang, K. Lin, T. Chen, H. Fu, and P. Chou, "Analysis of thermal resistance characteristics of power LED module," *IEEE Transactions on Electron Devices,* vol. 61, no. 1, pp. 105–109, Jan. 2014.
[28] X. Tao, H. Chen, S. Li, and S. Y. R. Hui, "A new noncontact method for the prediction of both internal themal resisitance and junction temperature of white light-emitting diodes," *IEEE Transactions on Power Electronics,* vol. 27, no. 4, pp. 2184–2192, Apr. 2012.
[29] T3Ster, Mentor Groaphics Corp., [Online] Available: https:// www.mentor.com/products/mechanical/micred/t3ster/.
[30] T3Ster Manual, "Thermal transient evaluation tool guide," 2010. [Online] Available: http://www.flotrend.com.tw/products/st3/t3ster/data/T3Ster_b.pdf.
[31] N. C. Sintamarean, F. Blaabjerg, H. Wang, F. Iannuzzo, and P. P. Rimmen, "Reliability oriented design tool for the new generation of grid connected PV-inverters," *IEEE Transactions on Power Electronics,* vol. 30, no. 5, pp. 2635–2644, May 2015.
[32] M. Miner, "Cumulative damage in fatigue," *Journal of Applied Mechanics,* vol. 12, pp. A159–A164, 1945.
[33] Bergquist Inc., "Power LED IMS substrates," 2015. [Online] Available: http://www.bergquistcompany.com/pdfs/LEDConfig20Sht_Re204.pdf.

This article has been accepted for publication in a future issue of this journal, but has not been fully edited. Content may change prior to final publication. Citation information: DOI 10.1109/TPEL.2016.2641010, IEEE Transactions on Power Electronics

10   IEEE TRANSACTIONS ON POWER ELECTRONICS, VOL. 1, NO. 1, JANUARY 2017

[34] T-Global Technology, "Lumi-Pad for LED configuration," 2015. [Online] Available: http://www.tglobaltechnology.com/LED-die-cuts/LP0005v01-Li98-0.25.pdf.

Frede Blaabjerg (S'86–M'88–SM'97–F'03) was with ABB-Scandia, Randers, Denmark, from 1987 to 1988. From 1988 to 1992, he was a Ph.D. Student with Aalborg University, Aalborg, Denmark. He became an Assistant Professor in 1992, Associate Professor in 1996, and Full Professor of power electronics and drives in 1998. His current research interests include power electronics and its applications such as in wind turbines, PV systems, reliability, harmonics and adjustable speed drives.

Dr. Blaabjerg has received 18 IEEE Prize Paper Awards, the IEEE PELS Distinguished Service Award in 2009, the EPE-PEMC Council Award in 2010, the IEEE William E. Newell Power Electronics Award 2014 and the Villum Kann Rasmussen Research Award 2014. He was an Editor-in-Chief of the IEEE Transactions on Power Electronics from 2006 to 2012. He is nominated in 2014, 2015 and 2016 by Thomson Reuters to be between the most 250 cited researchers in Engineering in the world.

Xiaohui Qu (S'08–M'10) received the B.Eng. and M.Eng. degrees in electrical engineering from the Nanjing University of Aeronautics and Astronautics, Nanjing, China, in 2003 and 2006, respectively, and the Ph.D. degree in power electronics from the Hong Kong Polytechnic University, Hong Kong, in 2010.

From February to May 2009, she was engaged as a Visiting Scholar at the Center for Power Electronics Systems, Virginia Tech, VA, USA. Since April 2010, she joined the School of Electrical Engineering, Southeast University, China, where she is currently an Associate Professor with research focus on power electronics. From January 2015 to January 2016, she was a Visiting Scholar with the Center of Reliable Power Electronics (CORPE), Aalborg University, Denmark. Her current research interests include LED lighting systems, wireless power transfer, and power electronics reliability.

Huai Wang (S'07–M'12) received the B.Eng. degree from the Huazhong University of Science and Technology, Wuhan, China, in 2007, and the Ph.D. degree from the City University of Hong Kong, Hong Kong, in 2012. He is currently an Associate Professor at the Center of Reliable Power Electronics (CORPE), Aalborg University, Denmark. He was a Visiting Scientist at ETH Zurich, Zurich, Switzerland, from August to September 2014, and at the Massachusetts Institute of Technology, Cambridge, MA, USA, from September to November 2013. He was at the ABB Corporate Research Center, Baden, Switzerland, in 2009. His research addresses the fundamental challenges in failure mechanism modelling and validation of power electronic components, and application issues in system-level predictability, condition monitoring, circuit architecture, and robustness design. He has contributed a few concept papers in the area of power electronics reliability, filed four patents in capacitive DC-link inventions, and co-edited a book.

Dr. Wang received the Richard M. Bass Outstanding Young Power Electronics Engineer Award from the IEEE Power Electronics Society in 2016, and the Green Talents Award from the German Federal Ministry of Education and Research in 2014. He is currently the Award Chair of the Technical Committee of the High Performance and Emerging Technologies, IEEE Power Electronics Society. He serves as an Associate Editor of IEEE Journal of Emerging and Selected Topics in Power Electronics and IEEE Transactions on Power Electronics.

Henry Shu-Hung Chung (M'95–SM'03–F'16) received the B.Eng. degree and the Ph.D. degree in electrical engineering both from the Hong Kong Polytechnic University, Hong Kong, in 1991 and 1994, respectively.

Since 1995 he has been with the City University of Hong Kong. He is currently Professor of the Department of Electronic Engineering and Director of the Centre for Smart Energy Conversion and Utilization Research. His research interests include renewable energy conversion technologies, lighting technologies, smart grid technologies, and computational intelligence for power electronic systems. He has edited one book, and authored eight research book chapters, and over 350 technical papers including 170 refereed journal papers in his research areas, and holds 35 patents. He was Chair of the Technical Committee of the High-Performance and Emerging Technologies, IEEE Power Electronics Society in 2010-2014. He is currently an Editor-in-Chief of the IEEE Power Electronics Letters, and an Associate Editor of the IEEE Transactions on Power Electronics, and IEEE Journal of Emerging and Selected Topics in Power Electronics. He has received numerous industrial awards for his invented energy saving technologies.

Xiaoqing Zhan (S'16) received the B.Eng. degree in electrical engineering from the Huazhong University of Science and Technology, Wuhan, China, in 2014. He is currently working toward the Ph.D. degree in Department of Electronic Engineering, the City University of Hong Kong, Kowloon, Hong Kong. His research interests include LED lighting system and power converters.